Recent Progresses in the Development of Solid-state Luminescent *o*-Carboranes with Stimuli Responsivity

Junki Ochi, Kazuo Tanaka* and Yoshiki Chujo

Department of Polymer Chemistry, Graduate School of Engineering, Kyoto University

Katsura, Nishikyo-ku, Kyoto 615-8510, Japan

tanaka@poly.synchem.kyoto-u.ac.jp

Tel: +81-75-383-2604

Fax: +81-75-383-2605

KEY WORDS: Carborane; aggregation-induced emission; chromism; solid-state luminescence; stimuli responsivity

ABSTRACT

o-Carborane is the cluster compound containing boron and adjacent carbon atoms. Recently, it has been revealed that *o*-carborane can be a versatile platform not only for suppressing aggregation-caused quenching and subsequently obtaining intense solid-state emission but also for developing stimuli-responsive luminochromic materials. In this mini-review, we introduce three kinds of fundamental photochemical properties, aggregation-induced emission, twisted intramolecular charge transfer in crystal and environment-sensitive excimer formation in solid. Based on these properties, several types of luminochromism, such as thermos-, vapo- and mechanochromism, have been discovered. Mainly according to results from recent studies, we illustrate mechanisms as well as unique luminescent behaviors of *o*-carborane derivatives.

1. Introduction

To realize future sensing technologies, such as wearable and/or film-type sensors, luminescent materials with stimuli responsivity are one of potential platforms. To fulfill this purposes, conjugated molecules have been regarded as a versatile building block for constructing stimuli-responsive luminescent materials because of intrinsic optical and electronic properties high environment sensitivity. Furthermore, it is possible to add unique functions by incorporating heteroatoms into electronic conjugation system. For instance, based on the high affinity between boron and fluoride, boron-containing conjugated materials are often applicable for luminescent fluoride sensors.[1] As another example regarding carborane, which is the main compound in this review, a ratiometric probe was accomplished based on the *nido*-carborane formation with the triphenylborane-modified compound.[2] From the stand point on effective usages of heteroatoms, we recently proposed the new concept for material design based on an “element-block”, which is the minimum functional unit containing heteroatom.[3–5] In this research field, several complexes and cluster compounds are found as a luminescent element-block. From these results, one of versatile boron element-block, *o*-carborane, is introduced in this review. Especially, recent progresses in the development of stimuli-responsive materials with solid-state luminescent properties are illustrated.

Carborane is an icosahedral cluster consisting of three-center two-electron bonds with the chemical formula $C_2B_{10}H_{12}$ (Scheme 1). Of the three kinds of isomers, *o*-carborane, which has the adjacent carbon atoms, has been particularly paid attention as a versatile platform for constructing functional solid-state luminescent dyes. Based on unique electronic properties, such as steric electronic conjugation and the position-dependent

electron donating and accepting ability,[6,7] various functions have been discovered from electronic interaction between carborane and π-conjugation. Therefore, *o*-carboranes have been applied in various fields as explained in the previous excellent reviews.[8–13] From the first report on aggregation-induced emission (AIE)-active polymers involving *o*-carborane, a wide variety of solid-state luminescent materials have been developed.[14] Now, it can be said that *o*-carborane is a building block for preparing functional solid-state luminescent materials because of its superior property for suppressing aggregation-caused quenching (ACQ). In this manuscript, we introduce a series of recent examples regarding solid-state luminescent *o*-carboranes with stimuli-responsivity and/or environment-sensitivity. Initially, three kinds of unique luminescent properties of *o*-carboranes, AIE (Section 2), twisted intramolecular charge transfer (TICT) in crystal (Section 3) and environment-sensitive excimer formation in solid (Section 4), are illustrated. The aryl-modified *o*-carboranes with crystallization-induced emission (CIE) and intense solid-state emission with quantitative efficiency are also introduced. Next, luminochromic behaviors in solid triggered by applying external stimuli and changing environmental factors are explained (Section 5). We also explain the unique intramolecular rotation of the *o*-carborane unit in crystal after photo-excitation. Basic chemistry and design strategies for these luminochromic materials are described.

2-1. *o*-Carborane derivatives with AIE properties

The AIE properties of *o*-carborane derivatives are explained. AIE was firstly discovered from the silole derivative in 2001, and so far various structures have been available.[15,16] In 2009, the AIE-active *o*-carboranes were found in the main-chain-type

conjugated polymers.[14] From this finding, the mechanistic studies have been performed with various *o*-carboranes, and the AIE properties can be explained mostly by the molecular motions at the *o*-carborane unit. In most of aryl-substituted *o*-carborane dyads, when the direction of the C–C bond is included in the π-plane, electronic interaction is hardly formed between *o*-carborane and the aryl moiety (Figure 1).[17] Therefore, the emission band is attributable to the transition from the locally-excited (LE) state of the aryl moiety.[18] In contrast, the *o*-carborane unit can work as an electron-acceptor when bonded at the carbon with the perpendicular distribution, where the C–C bond in *o*-carborane is vertically located toward the π-plane (Figure 1).[17] Therefore, intramolecular charge transfer (ICT) would occur after photo-excitation, followed by the significant emission band with the ICT character.[19,20] However, it should be noted that the ICT emission is not able to be obtained in solution. Due to molecular motions at the *o*-carborane in the excited state, deactivation rapidly occurs, followed by emission annihilation in solution.[21] In solid, these intramolecular motions would be suppressed because of structural restriction. Furthermore, the *o*-carborane unit can often suppress ACQ owing to steric hindrance. Therefore, solid-state emission is exhibited. Thus, AIE behaviors can be finally observed.

Some triphenylamine (TPA)-substituted *o*-carboranes were found to show AIE (Table 1, Scheme 2). In 2013, Inagi *et al.* synthesized the first TPA-substituted carborane **1**, and the typical AIE behavior was observed.[22] Very weak emission (Φ_{PL} = 0.007) was obtained in THF, while emission enhancement (Φ_{PL} = 0.05) was shown in THF/water (1/99). It is the typical AIE behavior. Kang *et al.* synthesized a series of TPA-substituted *o*-carboranes **2**–**9**[23–26] and carefully investigated the origin of AIE species using

transient absorption spectroscopy[25] and synchronous fluorescence spectroscopy[26]. It is noteworthy that the ICT state involving the *o*-carborane unit and the aryl moiety should have an important role in AIE. Other types of TPA-substituted carboranes, **10** and **11**, were reported by Lai *et al.*[27] *meta*-Substituted **10** and *para*-substituted **11** demonstrated AIE behaviors, similarly to the above compounds. Since **11** shows the emission band in the longer wavelength region than **10**, electronic interaction could be made through the *para*-substituted *o*-carboranes. By changing the number of the *o*-carborane substituent (**12**–**14**), AIE properties can be tuned.[28] By changing the number and position of the methyl substituents (**15**, **16**), environment sensitivity can be tuned.[29] The details will be mentioned later.

Tetraphenylethene (TPE) is one of conventional AIE-active molecules,[30] and intense emission in aggregate or solid was reported from some of TPE-substituted *o*-carboranes (Table 2, Scheme 3). Lu *et al.* prepared **17**–**21** and found that the replacement from the *o*-carborane unit to ethynylene or phenylene moieties in **21** resulted in weaker AIE efficiency.[31,32] This is because free rotation of the phenyl groups in the TPE moieties are effectively suppressed by the *o*-carborane unit. As another type of TPE substituents, **22** and **23** possessing stilbene linker was synthesized by Núñez and coworkers.[33] Some other TPE derivatives showed luminescence color changes by mechanical forces (**19**, **24**).[34,35] They will be discussed later.

In Table 3 and Scheme 3, a series of AIE-active materials having fluorene are listed. Carter *et al.* reported a series of carborane-containing polyfluorenes **25**–**27**.[36–40] Optoelectronic devices were fabricated with the emissive conjugated network involving

o-carborane for the first time. It was demonstrated that the carborane cage should be responsible for the improvement of charge carrier mobility by an order of magnitude.[38] In other paper, emission color can be tuned in a wide wavelength range by changing the introduction rate of the carborane unit.[40] Moreover, **25** showed vapochromic properties. Humphrey *et al.* synthesized various types of fluorene-substituted *o*-carboranes, and it was shown that compounds **28**–**35** have intense solid-state luminescent properties.[41,42] Accordingly, highly-efficient emission quantum yields were observed from **28** and **35** (Φ_{PL} = 0.95) in solid. Lee *et al.* demonstrated that flattened structures are favorable for obtaining clear AIE from the comparison biphenyl and fluorene-substituted compounds (**36**, **37**, **42**, **43**).[43] Planar conformation at the conjugated system and perpendicular distributions between the direction of C–C bond in *o*-carborane and π-planes are favorable for presenting AIE with the ICT character. Moreover, AIE efficiency was examined with spirobifluorene-tethered *o*-carboranes and *nido*-carboranes (**38**–**41**).[44] It was mentioned that the perpendicular distributions are also advantageous for obtaining higher efficiency of AIE. The details on the angle dependency will be discussed later.

Other types of AIE-active *o*-carborane derivatives are listed in Table 4 and Scheme 4. The influence on AIE properties were investigated by changing the substituents in *o*-carborane (**44**–**75**).[18,45–68] Among these compounds, solid-state excimer emission,[51] single-molecule white emission,[52] aggregation-induced electrochemiluminescence[53] and thermal-activated delayed fluorescence[54] were observed. A film-type sensor for fluoride anion was obtained with the modified *o*-carborane **65**.[55] The initial bluenish-green emissive film ($\lambda_{em,film}$ = 475 nm) exhibited color change to the longer wavelength region to yellow ($\lambda_{em,film}$ = 526 nm) by the treatment with

tetrabutylammonium fluoride. It is proposed that electronic conjugation should be drastically changed by the formation of dative bond between fluoride and tricoordinate boron at the substituent. The modified *o*-carboranes having stimuli-responsive luminochromism in solid have been reported (**76**–**85**).[61–68] The details are explained later. AIE as well as solid state emission were observed similarly to *o*-carboranes (**46**, **90**–**92**), while electronic conjugation is slightly extended through *m*-carborane and ACQ is often observed.[69,70] Commonly, *o*-carborane units should play critical roles in solid-state luminescence with the ICT character.

2-2. Vapochromic luminescent materials

AIE-active *o*-carboranes showed intriguing environment-sensitive luminochromism. For example, vapochromic luminescent properties, which represent luminochromism induced by fuming volatile organic compounds (VOCs), were exhibited from modified *o*-carboranes. Carter *et al.* reported a vapochromic property of the **25** from green (pristine) to red (after fumed by THF vapor).[37] It is noteworthy that the color shift correlated to the polarity of the solvent. With polar solvents, larger degree of red shifts was observed. Because charge separated states are generally stabilized under polar environment, red-shifted emission bands are observed in the ICT emission. Similarly to this general mechanism on solvatochromicity of the ICT emission, polar VOCs should induce red-shift. Moreover, **25** also responded to amine vapor through formation of the *nido*-species.

We prepared the bis-*o*-carborane-substituted aromatic rings (**46**, **90**–**99**) and found that some of crystal samples **90**, **91**, **92**, **95** and **96** exhibited CIE with good solid-state

emission efficiencies (Figure 2, Table 5, Scheme 5).[71–74] It is proposed that the two *o*-carboranes should efficiently disturb intermolecular interaction and subsequently induce intense solid-state emission. Furthermore, it was observed that luminochromism from the anthracene derivative **92** depended on the encapsulated solvent molecules, such as $CHCl_3$, CH_2Cl_2, and C_6H_6.[71] From the X-ray crystallography, it was proposed that relatively red-shifted emission was induced by increasing the π-stacking area at the anthracene moiety. Slight differences in molecular environment can be reflected as a luminescent color change. This molecule shows thermal isomerization to yield the *meta*-carborane-containing compound **94** (Figure 3).[75] The *meta*-carborane could work as a weak electron-acceptor without the angle dependency. Therefore, the electronic interaction between anthracene and the *meta*-carborane unit should be induced. As a result, solution emission should be observed.

3-1. TICT in crystal

The unique property in crystal originating from the sphere structure of *o*-carborane is illustrated. When we investigated emission properties of the anthracene–*o*-carborane dyad **100** (Table 5, Scheme 5) in 2-methyltetrahydrofuran at 77 K where molecular motions can be frozen, the typical emission band with the vibrational structure attributable to emission from the LE state of anthracene was observed (Figure 4a).[17] This means that the parallel distribution, where the direction of the C–C bond is involved in the π-plane, should be major in the ground state. On the other hand, at 298 K, the broad emission band attributable to the emission band with the ICT character was obtained, indicating that molecular rotation should occur in the excited state. Therefore, it was shown that the emission band should be generated through the TICT mechanism

(Figure 4b). Indeed, the good agreements were obtained from theoretical calculations: The parallel distribution is the most stable conformation in the ground state, meanwhile the twisted distribution is more stable than that of the parallel in the excited state. Next, we performed emission measurements in solid (Figure 4b). Surprisingly, the same results were obtained from the crystal sample to those from the solution despite that there is structural restriction. Under the frozen condition, only the LE emission was obtained, whereas the significant ICT emission was detected from the crystalline sample at 298 K. These data mean that the TICT process can proceed even in crystal.

To evaluate generality of TICT in crystal, the pyrene–*o*-carborane dyad **80** was synthesized and their optical properties were examined.[76] In summary, the TICT in crystal was also observed from the pyrene dyad. Furthermore, by introducing the substituent into the adjacent carbon atom to suppress the rotation, it was observed that emission efficiency can be drastically improved (**101**–**103**, **104**, **105**, Table 5, Scheme 5).[76,77] In particular, intense solid-state emission (Φ_{PL} > 0.99) with different emission color was accomplished by changing the aryl moiety. Furthermore, as mentioned above, blue-color luminescence with quantitative efficiencies was detected from the triads with the naphthalene moiety (**90**, **91**).[72] Similarly to conventional organic dyes, emission color can be tuned by the π-conjugation. Because of the substituent effect, intramolecular rotation in the excited state should be completely suppressed. Moreover, ACQ can be avoided in crystal because of the steric hindrance of *o*-carborane. Consequently, such intense solid-state luminescence can be obtained. From these results including quantum calculation and a series of emission properties, it is concluded that TICT is allowed in crystal of aryl-substituted *o*-carboranes.

The results from theoretical calculations represent the reason for intramolecular rotation after photo-excitation (Figure 5).[17] The LE and ICT emission can be induced from the parallel and perpendicular distribution, respectively. In the ground state, the parallel distribution is energetically stable, meanwhile the energy level is lifted by rotation. Finally, the perpendicular distribution has lower energy in the excited state. Additionally, owing to the sphere shape and low intermolecular interaction at *o*-carborane, a rotation barrier could be suppressed in the crystal packing. Thus, TICT can proceed in crystal. These data also mean that emission mechanism is switchable between LE and ICT by the molecular rotation at the connecting point with the *o*-carborane unit. Based on these characters, stimuli-responsive materials were obtained.

3-2. Thermochromic luminescent materials

To support solid-state TICT in the *o*-carborane dyads and to positively apply for environment-responsive luminochromism, we designed a series of the TPA dyads having variable numbers of methyl groups around the connecting point with the *o*-carborane unit ant the TPA moiety (**15**, **16**, Figure 6).[29] Because of steric hindrances of the substituents, it was presumed that a rotation barrier should be raised. As a result, critical temperature in thermochromic luminescent behaviors can be tuned. To evaluate validity of this idea, the dyads were prepared, and optical properties were analyzed.[29] All compounds showed solid-state emission and **16** presents clear dual emission property involving the LE and ICT emission bands.[52,79] Interestingly, red emission from the ICT transition of **16** was observed from the crystal at 298 K, meanwhile blue emission from the LE transition was induced by cooling at 77 K. From the evaluation of

energy barriers in the excited state with the Stevens–Ban plots, it was shown that the heights of energy barriers were significantly varied by the substituent effect. As a result, sensitivity in thermochromic luminescence can be tune.

From the optical measurements with the bis-phenyl-*o*-carborane-substituted aromatics (**95**–**99**), it was observed that rapid and reversible thermochromic luminescence occurred (Figure 7).[72,73] The aryl moieties were bent by the modification with the *o*-carborane substituents. Therefore, even in crystal, molecular tumbling should be allowed, and subsequently environment sensitivity was found. The anthracene dyads (**100**–**103**) and the bis-substituted compound **106** also show thermochromic luminescent properties.[77,78] Environmental alterations caused by heating followed by crystal packing releasing could induce emission color changes.

Other thermochromic luminescent materials are listed in Table 6. Guo and Jia *et al.* synthesized thermochromic compounds **76**–**79**.[61] It was observed that the introduction of alkyl linkages led to larger shift up to 32 nm. The following mechanisms were proposed: (1) Crystal packing was released by thermal motions at the alkyl linkages, and subsequently large degree of structural relaxation could be accepted. (2) The insets of alkyl linkages provided a featured transition from hard glassy state to soft rubbery state. Consequently, degree of structural relaxation was altered. Mechanochromic luminescence was also observed from **76**.[62] The details are illustrated later.

They also reported pyrene-substituted carboranes **80** and **81**.[63] These two compounds showed different thermochromic behaviors. Mono-substituted **80** has a

dual-emission property and the emission intensity ratio of dual emission was gradually changed. On the other hand, bis-substituted **81** with a unimodal emission band showed slight bathochromic shift as the temperature increased.

4. Environment-dependent excimer formation

As illustrated above, *o*-carborane can play a key role in suppressing ACQ, and ICT emission can be preserved in the solid state. Recently, it was observed that the *o*-carborane is effective for presenting solid-state excimer emission. In particular, formation of excimer emission was controllable by environmental factors in solid.

Stavrinou, Heeney and coworkers synthesized biscarborane-substituted chrysene **58**, which is a polycyclic aromatic hydrocarbon and shows excimer emission under the limited condition.[51] They found AIE, and it should be noted that excimer emission was detected in fluid. By increasing water content in the solution, not ICT but excimer emission was observed. Although the perpendicular distribution was formed, surprisingly, excimer formation can be facilitated in the *o*-carborane-involving π-conjugated system.

We also prepared the pyrene–*o*-carborane dyad with the ethynyl spacer **82** and examined optical properties (Figure 8).[64] In the absence of the *o*-carborane unit, ACQ was observed, while AIE with the ICT character was observed with the peak at 633 nm from the dyad. It should be emphasized that clear thermochromic luminescence was observed from orange to green by cooling at 77 K. From the emission spectra, not only the typical LE emission with the vibrational structure of pyrene but also a new emission

band was detected around 500 nm. From the peak position, this new emission band was assigned as excimer emission. From the quantum calculation, it was proposed that, similarly to previous molecules, TICT should proceed in solid, followed by ICT emission with the peak at 633 nm. By cooling, the molecular conformation was frozen at the initial state. Thus, LE emission should be observed owing to suppression of ACQ by the *o*-carborane unit. Therefore, excimer formation should be also facilitated in the solid sample. Finally, thermochromic luminescence from orange ICT emission to green LE and excimer emissions was realized.

The dyad **82** showed time-dependent aggregation-induced excimer emission in solution (Figure 9).[65] In the good solvent, the LE emission from the anthracene moiety was observed. Interestingly, emission intensity gradually increased and reached a plateau after the incubation for several hours even in the presence of a trace amount of water. By increasing water content, the increasing rate of emission was enhanced. According to the mechanistic study, it was revealed that molecular assembly was facilitated in the presence of water, followed by excimer emission. Based on this water-dependent emission enhancement through molecular assembly, we were able to construct the quantitative molecular probe for the water content in the sample with the wide detection range. From these data, we regard the aryl–ethynyl–*o*-carborane unit as a solid-state excimer-inducible “element-block”.

Next, to obtain solid-state excimer emission at ambient temperature, the heterocycle–*o*-carborane dyad **83** was designed (Figure 10).[66] As mentioned above, *o*-carborane has both an electron-accepting and donating characters at the carbon atoms and the distant

boron from carbon, respectively. From this fact, we presumed that each molecule could be aligned by the support of intermolecular interaction between the electron-accepting *o*-carborane and the nitrogen in the aryl moiety of the dyad. Accordingly, the acridine–*o*-carborane dyad showed excimer emission at room temperature not only in aggregation but also in crystal. In solution, blue emission attributable to the LE emission of the acridine moiety was observed. In aggregation and crystal, the broad emission band was observed in the yellow region. From the lifetime measurements, the longer value was obtained. In the absence of the *o*-carborane unit, excimer was not obtained in any phases. From X-ray crystallography, it was demonstrated that intermolecular C–H···N interaction is responsible for supporting alignment of the acridine moiety, implying that excimer should be formed in crystal. This result means that aggregation-induced excimer emission can be accomplished.

Morphology-dependent excimer formation is illustrated. The anthracene–*o*-carborane dyad **76** showed a tricolor turn-on luminescence in response to mechanical stimuli (Table 7).[62] The pristine powder gave bright blue emission. After being gently grinded, the sample exhibited bright yellow emission. Subsequently, the emission color was changed to pink under increased grinding force. In this manuscript, it is proposed that these emissions were assigned as LE, excimer, and TICT emission, respectively. The weak mechanical forces changed the packing mode in which the formation of excimers presenting yellow light is acceptable. By adding strong forces, further morphological change to amorphous should be induced, followed by observation of pink emission.

5. Mechanochromic luminescence

In the solid state, intermolecular interaction and packing strongly affect electronic properties. Therefore, if sufficient solid-state emission can be preserved, drastic changes in optical properties, such as emission intensity and/or color, are expected by phase transitions, such from crystal to amorphous. Based on this mechanism, mechanochromic luminescent properties, in which luminescent color can be changed by applying mechanical forces to crystal samples, have been accomplished with a series of *o*-carborane derivatives (Table 7).

Yan and Zhao *et al.* synthesized compound **86** including anthracene with the phenyl spacer and found that drastic emission color changes can be facilitated from blue to red by adding mechanical forces.[67] Interestingly, they also observed that reverse change to the initial color spontaneously proceeded within one minute at room temperature. Since an amorphous state is thermodynamically unstable, recrystallization should occur even at room temperature for a while. By removing the methyl group on the carbon atom in the *o*-carborane unit, loss of the mechanochromic property was observed, suggesting that newly-built CH–π interaction should inhibit generation of a metastable state by the mechanical treatment.

Nie *et al.* demonstrated the bis(naphthyl)phenyl-substituted carborane **85**, which showed bathochromic shift by 14 nm after grinding and resulted in presenting green fluorescence.[68] They also reported the mechanochromic luminescent compound **24** composed of the TPE moiety.[34] Huang *et al.* reported another TPE-functionalized carborane **19**.[35] Interestingly, the mono-substituted **59** shows white luminescent property, whereas the bis-substituted **85** exhibit stimuli-responsivity.[52,68] Diverse

properties can be obtained just by altering the combination of the functional units.

It is likely that degree of molecular tumbling in amorphous should be more vigorous than that in crystal due to weak packing. Indeed, lower emission efficiencies were often observed from the AIE-active *o*-carboranes (Table 5). Thereby, to obtain sensitive mechanochromic luminescent materials, loss of emission efficiency should be suppressed after adding mechanical forces. We found that the direct modification with two *o*-carborane units contributed to preserving emission efficiency of π-conjugated system even in amorphous as well as suppressing ACQ.[78] Based on the strategy for completely inhibiting molecular motions in **106** by the methyl modification at the adjacent carbon, we prepared **107** and detected dual-state emission not only in crystal but also in amorphous. Finally, it was shown that critical loss can be avoided during the mechanical treatment (before: λ_{em} = 493 nm, Φ_{PL} = 0.78; after: λ_{em} = 516 nm, Φ_{PL} = 0.61).

By removing one boron atom from carborane, *nido*-carborane is obtained. In general, the *nido*-carborane unit works as a strong electron-donor.[80] Therefore, AIE of aryl-modified *o*-carborane is not observed. In contrast, by removing another boron atom, the neutral compound, which is also called as *nido*-carborane, is produced. From this compound, electron-accepting ability is obtained, and solid-state luminescence with stimuli-responsivity was induced.[81] Helicene-connected *o*- and *nido*-carboranes without two boron atoms were simultaneously generated in a single reaction, and mechanochromic luminescence was detected only from the *nido*-carborane (Figure 11). The π-conjugation on the distorted structure of helicene should be anchored by the

nido-decaborane unit, and solid-state emission with stimuli responsiveness could be induced.

6. Conclusion

Because intermolecular interaction in the solid state is one of major emission annihilation processes, conventional materials have been made based on the strategy to isolate each molecule. In contrast, once solid-state luminescence can be assured, these interactions are able to be a versatile tool for regulating optical properties. According to experimental results described here, it can be said that the introduction of *o*-carborane is already the facile and promising strategy for obtaining solid-state luminescence. Thus, *o*-carborane derivatives are a potential platform for creating smart stimuli-responsive materials according to the preprogrammed design. To improve emission efficiency of organic luminescent dyes, rigid skeletons are favorable because energy-consumable molecular motions in the excited state can be suppressed. On the other hand, as described in this review, the molecular motions in the *o*-carborane unit play a key role in various luminescent behaviors. Owing to recent advances in theoretical calculations, motions of the excited molecules are predictable to some extent. Additionally, there are several experimental tools for estimating molecular dynamics after excitation. By utilizing these methods, exploration for new moving modes and their control are a significant technology for creating next generation of luminescent materials.

REFERENCES

[1] N. Matsumi, K. Naka, Y. Chujo, *J. Am. Chem. Soc*. **1998**, *120*, 10776–10777.

[2] K. C. Song, H. Kim, K. M. Lee, Y. S. Lee, Y. Do, M. H. Lee, *Dalton Trans*. **2013**, *42*, 2351–2354.

[3] Y. Chujo, K. Tanaka, *Bull. Chem. Soc. Jpn*. **2015**, *88*, 633-643.

[4] M. Gon, K. Tanaka, Y. Chujo, *Polym. J*. **2018**, *50*, 109–126.

[5] M. Gon, K. Tanaka, Y. Chujo, *Bull. Chem. Soc. Jpn*. **2019**, *92*, 7–18.

[6] K. Kokado, Y. Chujo, *J. Org. Chem*. **2011**, *76*, 316–319.

[7] A. M. Spokoyny, C. W. Machan, D. J. Clingerman, M. S. Rosen, M. J. Wiester, R. D. Kennedy, C. L. Stern, A. A. Sarjeant, C. A. Mirkin, *Nat. Chem*. **2011**, *3*, 590–596.

[8] V. I. Bregadze, *Chem. Rev*. **1992**, *92*, 209−223.

[9] M. Scholz, E. Hey-Hawkins, *Chem. Rev*. **2011**, *111*, 7035−7062.

[10] R. Núñez, M. Terrés, A. Ferrer-Ugalde, F. F. d. Biani, F. Teixidor, *Chem. Rev*. **2016**, *116*, 14307−14378.

[11] F. Issa, M. Kassiou, L. M. Rendina, *Chem. Rev*. **2011**, *111*, 5701−5722.

[12] R. Núñez, I. Romero, F. Teixidor, C. Viñas, *Chem. Soc. Rev*. **2016**, *45*, 5147−5173.

[13] R. N. Grimes, *Carboranes, 2nd ed., Academic Press, Amsterdam*, **2011**, 301–540.

[14] K. Kokado, Y. Chujo, *Macromolecules* **2009**, *42*, 1418–1420.

[15] J. Luo, Z. Xie, J. W. Lam, L. Cheng, H. Chen, C. Qiu, H. S. Kwok, X. Zhan, Y. Liu, D. Zhu, B. Z. Tang, *Chem. Commun.* **2001**, 1740–1741.

[16] J. Mei, N. L. C. Leung, R. T. K. Kwok, J. W. Y. Lam, B. Z. Tang, *Chem. Rev*.

2015, *115*, 11718−11940.

[17] H. Naito, K. Nishino, Y. Morisaki, K. Tanaka, Y. Chujo, *Angew. Chem. Int. Ed.* **2017**, *56*, 254−259.

[18] K. Nishino, K. Hashimoto, K. Tanaka, Y. Morisaki, Y. Chujo, *Tetrahedron Lett*. **2016**, *57*, 2025−2028.

[19] Z. Wang, P. Jiang, T. Wang, G. J. Moxey, M. P. Cifuentes, C. Zhang, M. G. Humphrey, *Phys. Chem. Chem. Phys*. **2016**, *18*, 15719–15726.

[20] S. Kwon, K.-R. Wee, Y.-J. Cho, S. O. Kang, *Chem. Eur. J*. **2014**, *20*, 5953–5960.

[21] K. Tanaka, K. Nishino, S. Ito, H. Yamane, K. Suenaga, K. Hashimoto, Y. Chujo, *Faraday Discuss*. **2017**, *196*, 31–42.

[22] S. Inagi, K. Hosoi, T. Kubo, N. Shida, T. Fuchigami, *Electrochemistry* **2013**, *81*, 368–370.

[23] S.-Y. Kim, Y.-J. Cho, G. F. Jin, W.-S. Han, H.-J. Son, D. W. Cho, S. O. Kang, *Phys. Chem. Chem. Phys*. **2015**, *17*, 15679–15682.

[24] Y. J. Cho, S. Y. Kim, M. Cho, W. S. Han, H. J. Son, D. W. Cho, S. O. Kang, *Phys. Chem. Chem. Phys*. **2016**, *18*, 9702–9708.

[25] M. R. Son, Y. J. Cho, S. Y. Kim, H. J. Son, D. W. Cho, S. O. Kang, *Phys. Chem. Chem. Phys*. **2017**, *19*, 24485–24492.

[26] S. Y. Kim, J. D. Lee, Y. J. Cho, M. R. Son, H. J. Son, D. W. Cho, S. O. Kang, *Phys. Chem. Chem. Phys*. **2018**, *20*, 17458–17463.

[27] Y. Wan, J. Li, X. Peng, C. Huang, Q. Qi, W. Y. Lai, W. Huang, *RSC Adv*. **2017**, *7*, 35543–35548.

[28] K. Nishino, K. Uemura, K. Tanaka, Y. Chujo, *Molecules* **2017**, *22*, 2009−2018.

[29] K. Nishino, K. Tanaka, Y. Chujo, *Asian J. Org. Chem.* **2019**, 8, 2228–2232.

[30] H. Tong, Y. Hong, Y. Dong, M. Häußler, J. W. Y. Lam, Z. Li, Z. Guo, Z. Guo, B. Z. Tang, *Chem. Commun*. **2006**, 3705–3707.

[31] X. Li, Y. Yin, H. Yan, C. Lu, *Chem. Asian J*. **2017**, *12*, 2207–2210.

[32] Y. Yin, X. Li, S. Yan, H. Yan, C. Lu, *Chem. Asian J*. **2018**, *13*, 3155–3159.

[33] J. Cabrera-González, S. Bhattacharyya, B. Milián-Medina, F. Teixidor, N. Farfán, R. Arcos-Ramos, V. Vargas-Reyes, J. Gierschner, R. Núñez, *Eur. J. Inorg. Chem*. **2017**, *2017*, 4575–4580.

[34] Y. Nie, H. Zhang, J. Miao, X. Zhao, Y. Li, G. Sun, *J. Organomet. Chem*. **2018**, *865*, 200–205.

[35] J. Li, C. Yang, X. Peng, Y. Chen, Q. Qi, X. Luo, W.-Y. Lai, W. Huang, *J. Mater. Chem. C* **2018**, *6*, 19–28.

[36] J. J. Peterson, M. Werre, Y. C. Simon, E. B. Coughlin, K. R. Carter, *Macromolecules* **2009**, *42*, 8594–8598.

[37] J. J. Peterson, A. R. Davis, M. Werre, E. B. Coughlin, K. R. Carter, *ACS Appl. Mater. Interfaces* **2011**, *3*, 1796–1799.

[38] A. R. Davis, J. J. Peterson, K. R. Carter, *ACS Macro Lett*. **2012**, *1*, 469–472.

[39] K. L. Martin, A. Krishnamurthy, J. Strahan, E. R. Young, K. R. Carter, *J. Phys. Chem. A* **2019**, *123*, 1701–1709.

[40] K. L. Martin, J. N. Smith, E. R. Young, K. R. Carter, *Macromolecules* **2019**, *52*, 7951–7960.

[41] Z. Wang, T. Wang, C. Zhang, M. G. Humphrey, *Phys. Chem. Chem. Phys*. **2017**, *19*, 12928–12935.

[42] Z. Wang, T. Wang, C. Zhang, M. G. Humphrey, *ChemPhotoChem* **2018**, *2*, 369–379.

[43] N. Shin, S. Yu, J. H. Lee, H. Hwang, K. M. Lee, *Organometallics* **2017**, *36*, 1522–1529.

[44] S. Kim, J. H. Lee, H. So, J. Ryu, J. Lee, H. Hwang, Y. Kim, M. H. Park, K. M. Lee, *Chem. Eur. J*. **2020**, *26*, 548–557.

[45] H. J. Bae, H. Kim, K. M. Lee, T. Kim, Y. S. Lee, Y. Do, M. H. Lee, *Dalton Trans*. **2014**, *43*, 4978–4985.

[46] J. H. Lee, H. Hwang, K. M. Lee, *J. Organomet. Chem*. **2016**, *825–826*, 69–74.

[47] D. K. You, J. H. Lee, B. H. Choi, H. Hwang, M. H. Lee, K. M. Lee, M. H. Park, *Eur. J. Inorg. Chem*. **2017**, *2017*, 2496–2503.

[48] Y. Chen, J. Guo, X. Wu, D. Jia, F. Tong, *Dye Pigments* **2018**, *148*, 180–188.

[49] X. Yang, B. Zhang, S. Zhang, G. Li, L. Xu, Z. Wang, P. Li, Y. Zhang, Z. Liu, G. He, *Org. Lett*. **2019**, *21*, 8285–8289.

[50] S. Choi, H.-E. Lee, C. H. Ryu, J. Lee, J. Lee, M. Yoon, Y. Kim, M. H. Park, K. M. Lee, M. Kim, *Chem. Commun*. **2019**, *55*, 11844–11847.

[51] A. V. Marsh, N. J. Cheetham, M. Little, M. Dyson, A. J. P. White, P. Beavis, C. N. Warriner, A. C. Swain, P. N. Stavrinou, M. Heeney, *Angew. Chem. Int. Ed*. **2018**, *57*, 10640–10645.

[52] D. Tu, P. Leong, S. Guo, H. Yan, C. Lu, Q. Zhao, *Angew. Chem. Int. Ed*. **2017**, *56*, 11370–11374.

[53] X. Wei, M. Zhu, Z. Cheng, M. Lee, H. Yan, C. Lu, J. Xu, *Angew. Chem. Int. Ed*. **2019**, *58*, 3162–3166.

[54] R. Furue, T. Nishimoto, I. S. Park, J. Lee, T. Yasuda, *Angew. Chem. Int. Ed*. **2016**, *55*, 7171–7175.

[55] B. H. Choi, J. H. Lee, H. Hwang, K. M. Lee, M. H. Park, *Organometallics* **2016**,

35, 1771–1777.

[56] X. Wu, J. Guo, Y. Quan, W. Jia, D. Jia, Y. Chen, Z. Xie, *J. Mater. Chem. C* **2018**, *6*, 4140–4149.

[57] E. Berksun, I. Nar, A. Atsay, İ. Özçeşmeci, A. Gelir, E. Hamuryudan, *Inorg. Chem. Front*. **2018**, *5*, 200–207.

[58] A. Ferrer-Ugalde, J. Cabrera-González, E. J. Juárez-Pérez, F. Teixidor, E. Pérez-Inestrosa, J. M. Montenegro, R. Sillanpää, M. Haukka, R. Núñez, *Dalton Trans*. **2017**, *46*, 2091–2104.

[59] L. Weber, J. Kahlert, L. Böhling, A. Brockhinke, H.-G. Stammler, B. Neumann, R. A. Harder, P. J. Low, M. A. Fox, *Dalton Trans*. **2013**, *42*, 2266–2281.

[60] L. Böhling, A. Brockhinke, J. Kahlert, L. Weber, R. A. Harder, D. S. Yufit, J. A. K. Howard, J. A. H. MacBride, M. A. Fox, *Eur. J. Inorg. Chem*. **2016**, *2016*, 403–412.

[61] X. Wu, J. Guo, W. Jia, J. Zhao, D. Jia, H. Shan, *Dye Pigment* **2019**, *162*, 855–862.

[62] X. Wu, J. Guo, Y. Cao, J. Zhao, W. Jia, Y. Chen, D. Jia, *Chem. Sci*. **2018**, *9*, 5270–5277.

[63] X. Wu, J. Guo, J. Zhao, Y. Che, D. Jia, Y. Chen, *Dye Pigment* **2018**, *154*, 44–51.

[64] K. Nishino, H. Yamamoto, K. Tanaka, Y. Chujo, *Asian J. Org. Chem*. **2017**, *6*, 1818−1822.

[65] K. Nishino, H. Yamamoto, K. Tanaka, Y. Chujo, *Chem. Asian J*. **2019**, *14*, 1577−1581.

[66] J. Ochi, K. Tanaka, Y. Chujo, *Eur. J. Org. Chem*. **2019**, 2984−2988.

[67] D. Tu, P. Leong, Z. Li, R. Hu, C. Shi, K. Y. Zhang, H. Yan, Q. Zhao, *Chem.*

Commun. **2016**, *52*, 12494–12497.

[68] Y. Nie, H. Zhang, J. Miao, Y. Wang, Y. Li, D. Tu, H. Yan, G. Sun, X. Jiang, *Inorg. Chem. Commun*. **2019**, *106*, 1–5.

[69] J. Cabrera-González, C. Viñas, M. Haukka, S. Bhattacharyya, J. Gierschner, R. Núñez, *Chem. Eur. J*. **2016**, *22*, 13588–13598.

[70] M. Chaari, Z. Kelemen, D. Choquesillo-Lazarte, N. Gaztelumendi, F. Teixidor, C. Viñas, C. Nogués, R. Núñez, *Biomater. Sci*. **2019**, *7*, 5324–5337.

[71] H. Naito, Y. Morisaki, Y. Chujo, *Angew. Chem. Int. Ed*. **2015**, *54*, 5084–5087.

[72] H. Naito, K. Nishino, Y. Morisaki, K. Tanaka, Y. Chujo, *Chem. Asian J*. **2017**, *12*, 2134−2138.

[73] K. Nishino, K. Uemura, K. Tanaka, Y. Morisaki, Y. Chujo, *Eur. J. Org. Chem*. **2018**, *2018*, 1507−1512.

[74] K. Nishino, K. Tanaka, Y. Morisaki, Y. Chujo, *Chem. Asian J*. **2019**, *14*, 789−795.

[75] H. Naito, K. Uemura, Y. Morisaki, K. Tanaka, Y. Chujo, *Eur. J. Org. Chem*. **2018**, *2018*, 1885−1890.

[76] K. Nishino, H. Yamamoto, K. Tanaka, Y. Chujo, *Org. Lett*. **2016**, *18*, 4064−4067.

[77] H. Naito, K. Nishino, Y. Morisaki, K. Tanaka, Y. Chujo, *J. Mater. Chem. C* **2017**, *5*, 10047−10054.

[78] H. Mori, K. Nishino, K. Wada, Y. Morisaki, K. Tanaka, Y. Chujo, *Mater. Chem. Front*. **2018**, *2*, 573–579.

[79] K. Nishino, K. Uemura, K. Tanaka, Y. Chujo, *New J. Chem*. **2018**, *16*, 4210−4214.

[80] K. Nishino, Y. Morisaki, K. Tanaka, Y. Chujo, *New J. Chem*. **2017**, *15*,

10550−10554.

[81] K. Nishino, K. Hashimoto, K. Tanaka, Y. Morisaki, Y. Chujo, *Sci. China Chem*. **2018**, *61*, 940−946.

FIGURES AND TABLES

Table 1. Optical properties of TPA-modified *o*-carboranes with AIE property

compound	$\lambda_{em,solution}$ [nm]	$\Phi_{PL,solution}$	$\lambda_{em,AIE}$ [nm]	$\Phi_{PL,AIE}$	ref.
1	430	0.007	570	0.05	[22]
2	382	–	620	1.19×10^{-3}	[23,25]
3	448	–	683	–	[23]
4	366,454	–	661	1.195×10^{-3}	[23]
5	398	0.21×10^{-3}[26]	577	0.635	[25,26]
6	430	–	570	–	[24]
7	432	–	577	–	[24]
8	425[a]	3.67×10^{-3}	610[a]	6.65×10^{-3}	[25]
9	388	0.008	562	0.061	[26]
10	425[a]	–	574	–	[27]
11	425[a]	–	600[a]	–	[27]
12	374, 557	<0.01	372,635	0.04	[28,29]
13	362, 541	<0.01	623	0.30	[28]
14	358, 516	<0.01	602	0.25	[28]
15	548	< 0.01	589	0.65	[29]
16	389, 609	< 0.01	382, 637	0.60	[29]

[a]Estimated from the spectra.

Table 2. Optical properties of TPE-modified *o*-carboranes with AIE property

compound	$\lambda_{em,solution}$ [nm]	$\Phi_{PL,solution}$	$\lambda_{em,AIE}$ [nm]	$\Phi_{PL,AIE}$	ref.
17	–	–	452	0.18	[31]
18	–	–	533	0.58	[31]
19	–	–	553[31],522[35]	0.63[31],0.95[35]	[31,35]
20	–	–	452	0.34	[31]
21	–	–	560	0.55	[32]
22	563	0.12	559	0.51	[33]
23	563	0.15	561	0.56	[33]
24	428	–	483	1.00	[34]

Table 3. Optical properties of fluorene-modified carboranes with AIE property

compound	$\lambda_{em,solution}$ [nm]	$\Phi_{PL,solution}$	$\lambda_{em,AIE}$ [nm]	$\Phi_{PL,AIE}$	ref.
25	569[38]	0.3[39]	520[36],563[38]	0.4[39]	[36–39]
26	602	–	570	–	[38]
27[a]	410,430,595	0.17,0.24	410,430,595	0.39	[40]
28	399	<0.01	502	0.95	[41]
29	475	<0.01	496	0.75	[41]
30	464	<0.01	497	0.94	[41]
31	411, 435, 593	0.03	528	0.85	[42]
32	411, 435, 636	0.02	572	0.34	[42]
33	411, 435, 628	0.02	563	0.43	[42]
34	411, 435	0.03	546	0.42	[42]
35	411, 435	0.04	528	0.95	[42]
36	503	0.009	490	0.366	[43]
37	366	0.060	479	0.368	[43]
38	389	389,499	0.127	0.133,0.165	[44]
39	389	389	0.119	0.150	[44]
40	371,578	373,538	0.182	0.426	[44]
41	388	375	<0.01	<0.01	[44]

[a]m=20, n=80.

Table 4. Optical properties of modified *o*-carboranes with AIE property

compound	$\lambda_{em,solution}$ [nm]	$\Phi_{PL,solution}$	$\lambda_{em,AIE}$ [nm]	$\Phi_{PL,AIE}$	ref.
42	386	0.245	383	0.336	[43]
43	363	0.040	460	–	[43]
44	378,400,426,453	0.007		0.043	[18]
45	510 (77 K)	–	478	–	[45]
46[a]	520 (77 K)	–	513	–	[45,70]
47	539 (77 K)	–	511	–	[45]
48	639 (77 K)	–	631	–	[45]
49	355	0.009	500	–	[46]
50	352	0.040	539	0.097	[47]
51	–	0.007	596	0.357	[48]
52	–	0.004	621	0.250	[48]
53	–	0.006	637	0.257	[48]
54	–	0.006	638	0.265	[48]
55	–	–	548	–	[49]
56	440	–	538	0.115	[49]
57	–	–	550[c]	–	[50]
58	657,657	0.031	585	0.32	[51]
59	376	0.039	400,550[c]	0.46	[52]
60	375	<0.001	540[c]	0.018	[53]
61	–	<0.001	550[c]	0.012	[53]
62	346, 467	0.03	557	0.97	[54]
63	533	0.03	624	0.55	[54]
64	350	0.01	571	0.94	[54]
65	376	0.18	493	–	[55]
66	460, 484	0.031	572	0.070	[56]
67	461, 486	0.009	528	0.429	[56]
68	462, 485	0.008	529	0.316	[56]
69	654	–	654	–	[57]
70	355	0.024	540[c]	–	[58]
71	371	0.029	520	–	[58]
72	646~757	<0.06	523~654	0.05~0.70	[59]
73	346	<0.001	612	0.02	[60]
74	348	0.04	537	0.07	[60]
75	442	<0.001	476	0.09	[60]
76	402, 434	0.005	441	0.043	[61,62]
77	401, 431, 590	0.008	575	0.360	[61]
78	401, 428, 607	0.007	566	0.408	[61]
79	401, 430, 612	0.007	555	0.514	[61]
80[b]	387, 403, 592	0.049	594	0.353	[63,75]
81	387, 405, 452, 638	0.005	644	0.132	[63]
82	389, 409	<0.01	622	0.09	[64,65]
83	424, 448	0.06	574	0.23	[66]
84	425[c]	0.02	425, 600[c]	–	[67]
85	–	–	491	–	[68]
86	355[c]	0.05	460[c]	0.12	[69]
87	355	0.07	462	0.38	[69]
88	–	0.08	450	0.30	[69]
89	352	0.08	445	0.17	[69]

[a]Listed the data from ref. 43.
[b]Listed the data from ref. 61.
[c]Estimated from the spectra.

Table 5. Modified *o*-carboranes with high emission efficiencies

compound	THF		THF/water=1/99		crystal		ref.
	λ_{em} (nm)	Φ_{PL}[a]	λ_{em} (nm)	Φ_{PL}	λ_{em} (nm)	Φ_{PL}	
46[a]	–	–	322	–	397	–	[45,72]
90	549	0.04	501	0.23	486	>0.99	[72]
91	530	<0.01	491	0.53	468	>0.99	[72]
92	647	<0.01	643	0.08	613	0.81	[71,72]
93	652	0.19	642	0.38	632	0.59	[75]
94	–	–	759	0.01	742	<0.01	[72]
95	682	0.12	638	0.23	617	0.90	[73]
96	670	0.03	627	0.43	611	0.67	[74]
97	698	0.12	615	0.72	591	0.94	[73,74]
98	686	0.02	628	0.25	563	0.64	[74]
99	727	<0.01	648	0.17	645	0.32	[74]
100	459, 609	0.02	598	0.18	606	0.38	[17,77]
101	624	<0.01	624	0.21	582	0.81	[77]
102	588	<0.01	587	0.29	563	>0.99	[77]
103	614	0.55	605	0.37	604	0.97	[77]
80[b]	401, 631	0.16	596	0.40	618	0.80	[63,76]
104	611	0.41	584	0.60	545	0.99	[76]
105	401, 632	0.19	599	0.73	579	0.99	[76]
106	371, 566	0.30	538	0.36	537	0.57	[78]
107	540	0.84	542	0.81	493	0.78	[78]

[a]Listed the data from ref. 68.
[b]Listed the data from ref. 72.

Table 6. Optical properties of modified *o*-carboranes with thermochromic luminescent properties

compound	$\Delta\lambda_{em}$ [nm]	ref.
12	14 (77~298 K)	[29]
15	2 (77~298 K)	[29]
16	248 (77~298 K)	[29]
76	4 (77~333 K)	[61,62]
77	2 (77~333 K)	[61]
78	16 (77~333 K)	[61]
79	32 (77~333 K)	[61]
80	125 (77~333 K)[a]	[63]
81	25 (77~333 K)[a]	[63]
83	117 (77~298 K)	[64]
95	9 (298~473 K)	[74]
96	5 (298~473 K)	[74]
97	19 (298~473 K)	[74]
98	21 (298~473 K)	[74]
99	18 (298~473 K)	[74]
100	3 (298~498 K)	[77]
101	33 (298~498 K)	[77]
102	16 (298~498 K)	[77]
103	12 (298~498 K)	[77]
106	20 (275~353 K)	[78]

[a]Estimated from the spectra.

Table 7. Optical properties of modified *o*-carboranes with mechanochromic luminescent properties

compound	$\Delta\lambda_{em}$ [nm]	ref.
19	25	[35]
24	16	[34]
76	90,185	[63]
84	0,150[a]	[67]
85	14	[68]
107	23	[78]

[a]Estimated from the spectra.

Scheme 1. Chemical structures of carborane isomers

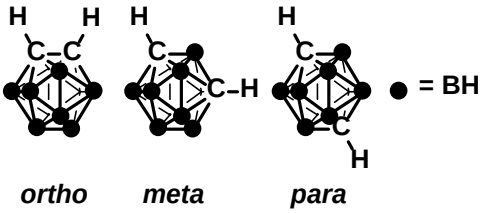

Scheme 2. Chemical structures of TPA-modified *o*-carboranes

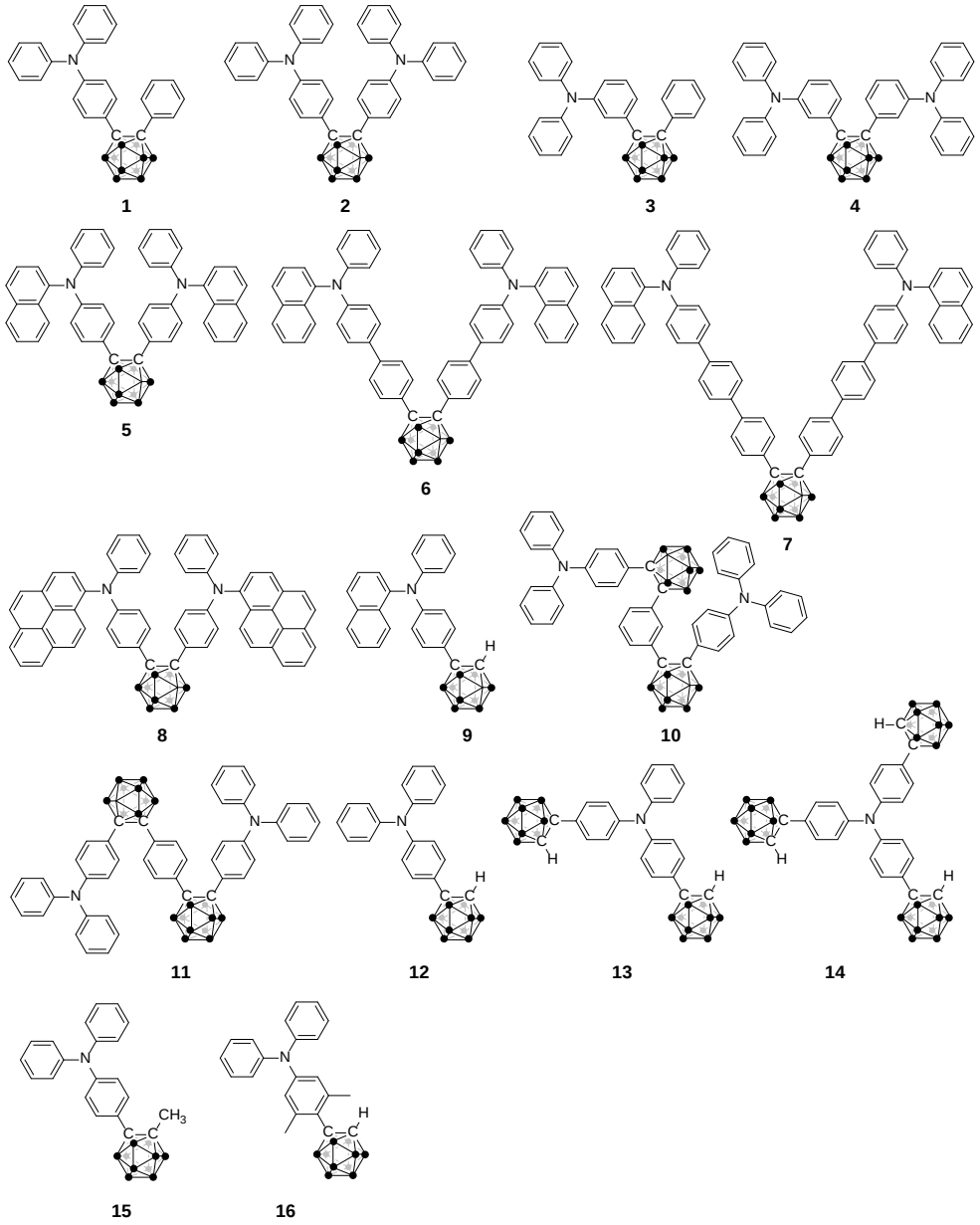

Scheme 3. Chemical structures of TPE- and fluorene-modified *o*-carboranes

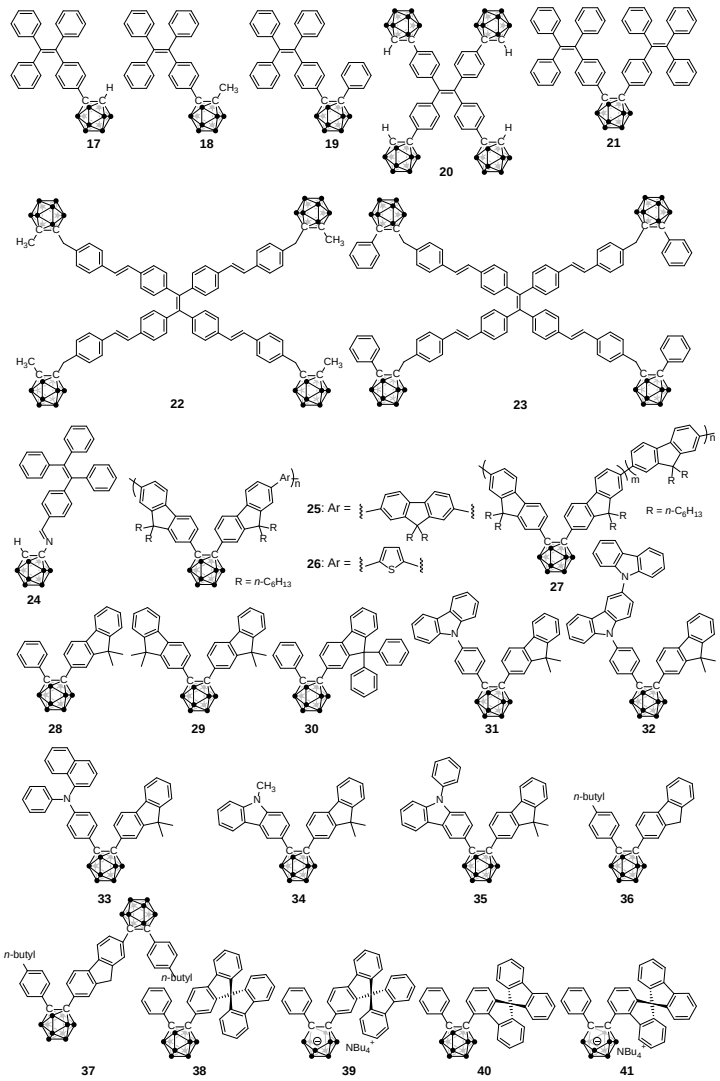

Scheme 4. Chemical structures of other AIE-active carboranes

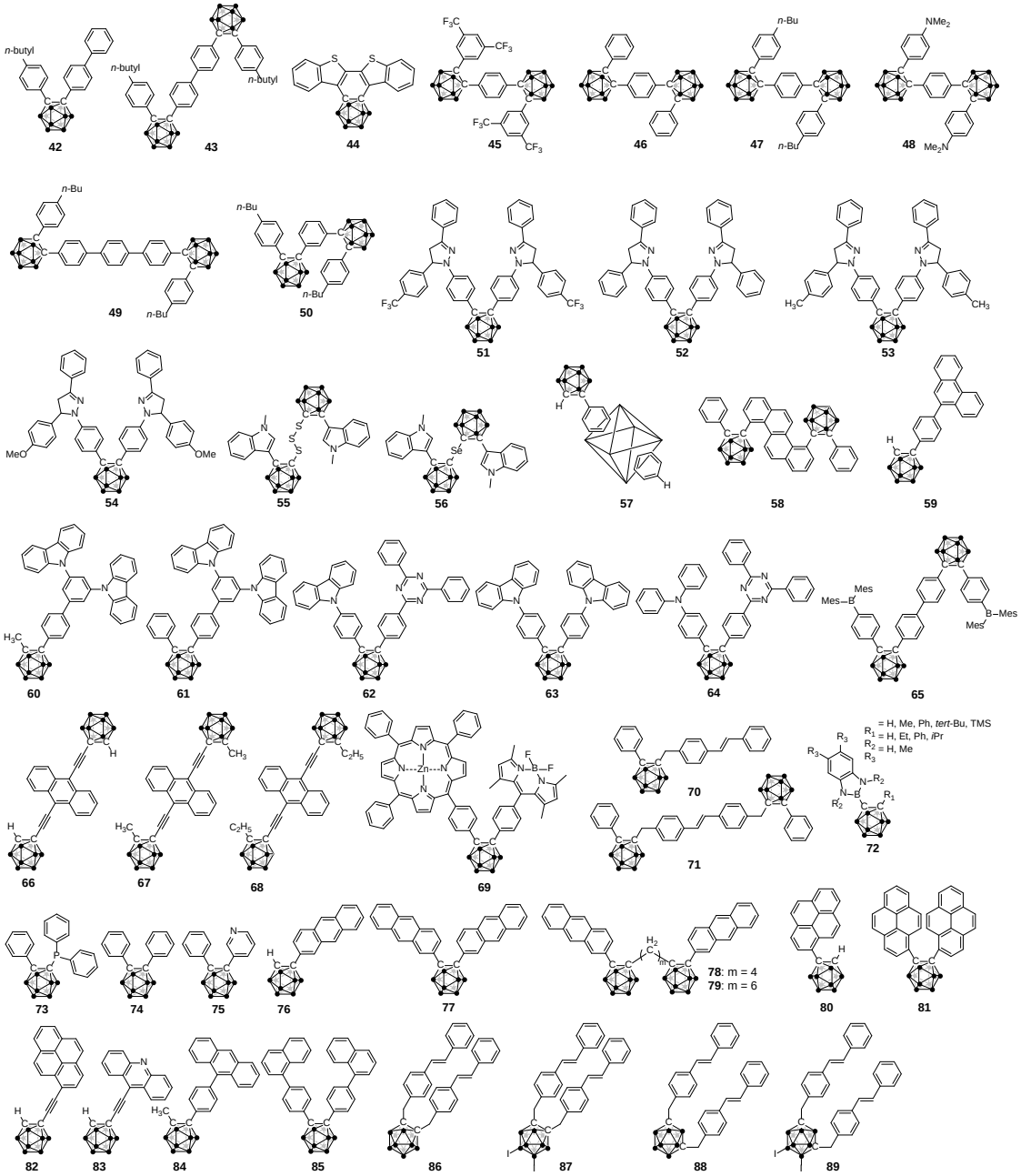

Scheme 5. Chemical structures of modified *o*-carboranes with efficient solid-state luminescent properties

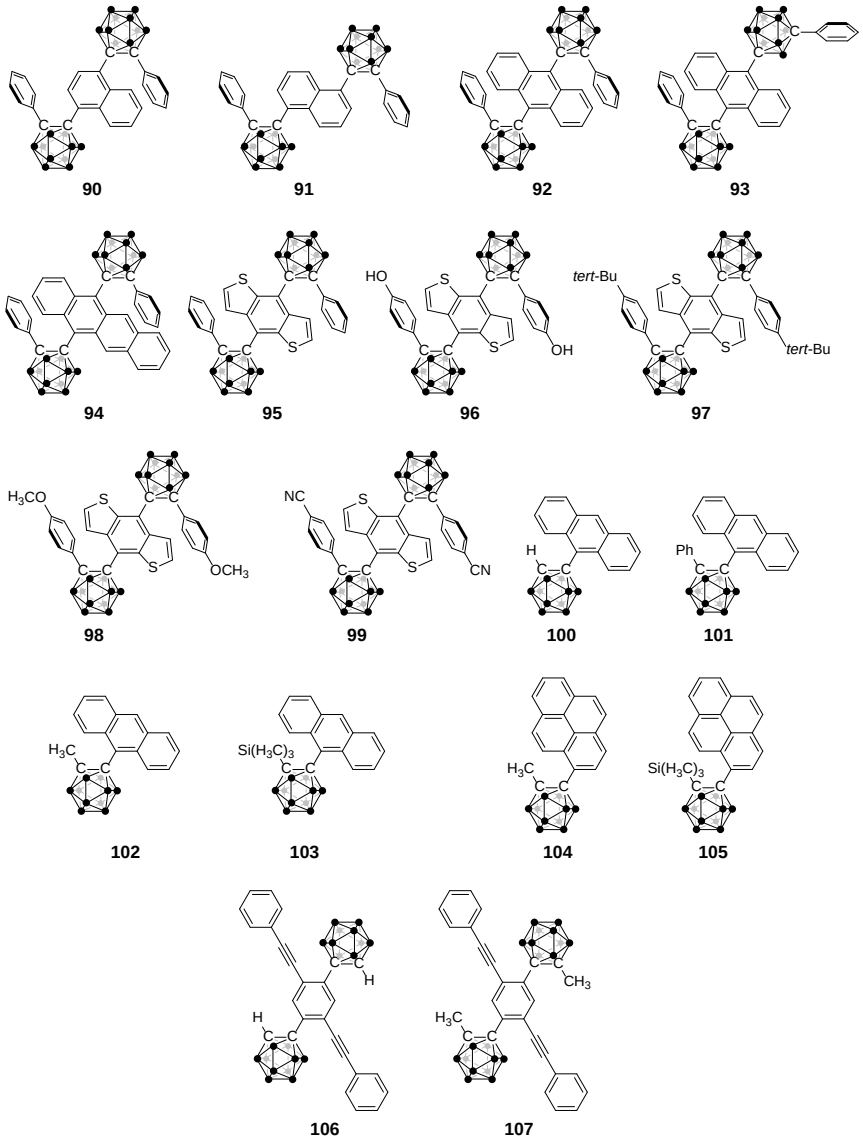

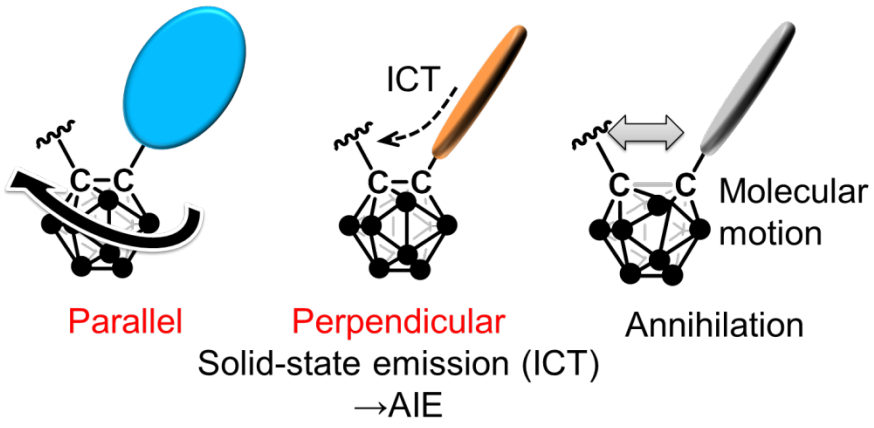

Figure 1. Photochemistry of aryl–*o*-carborane dyads.

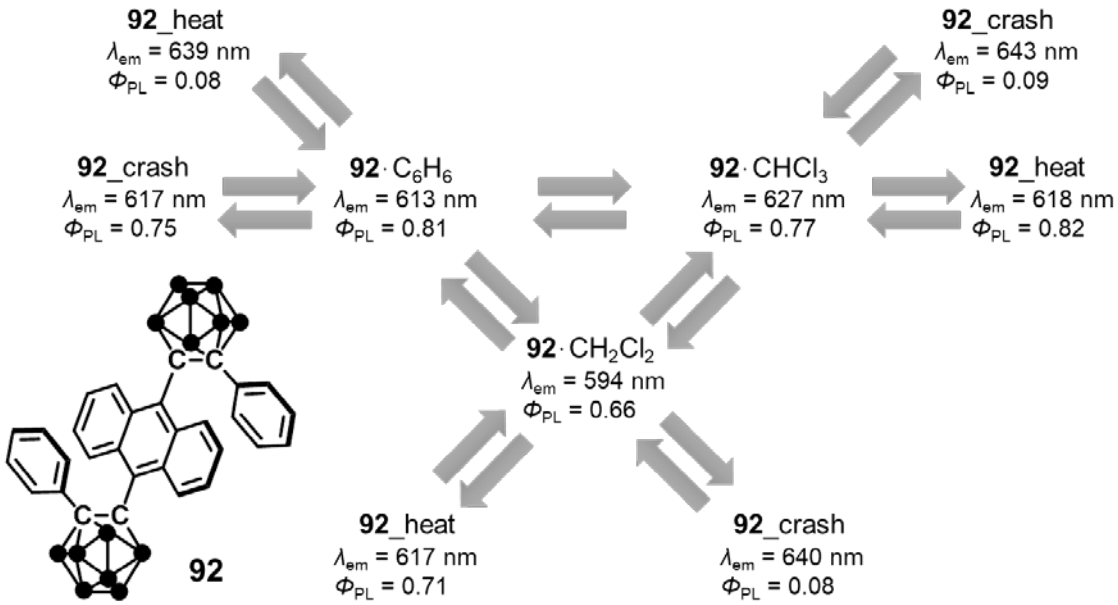

Figure 2. Multichromic luminescent properties of bis-*o*-carborane-substituted anthracene **92**.

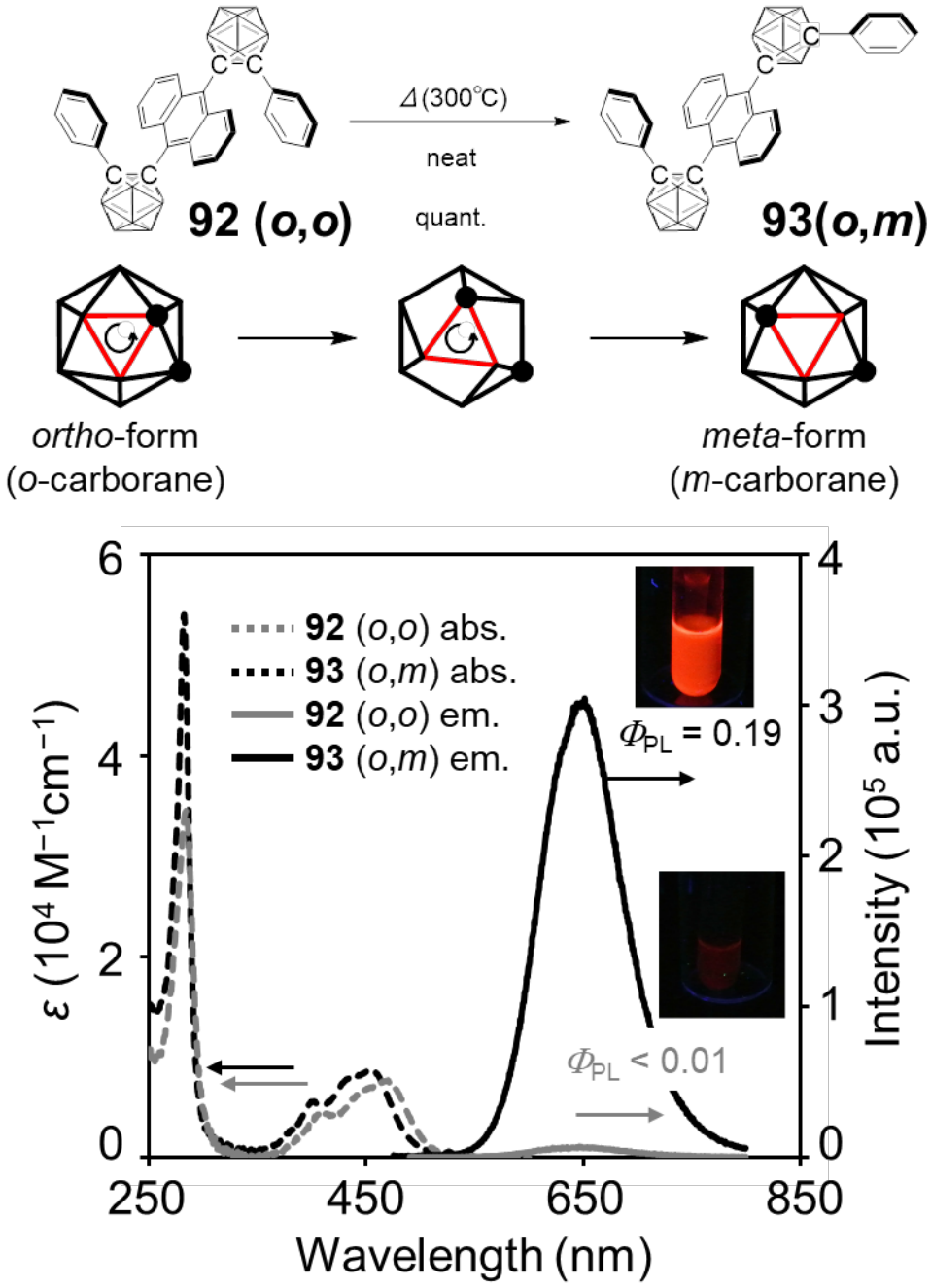

Figure 3. Thermal rearrangement in **92** and optical spectra of the product **93**. Reprinted with permission from ref 75. Copyright 2018 Wiley-VCH Verlag GmbH & Co. KGaA.

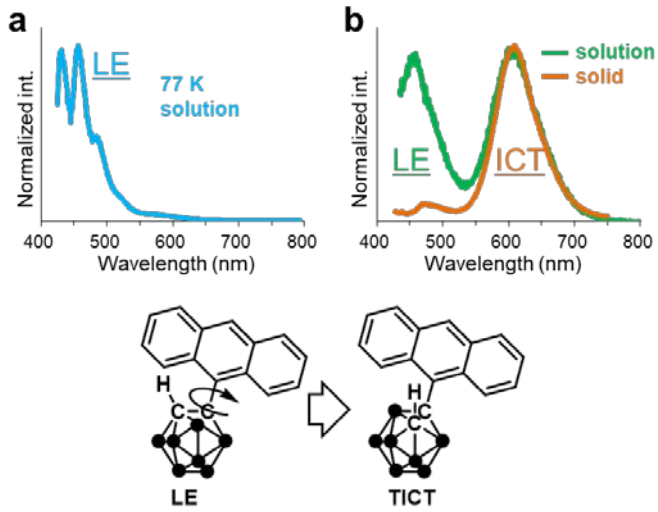

Figure 4. Luminescent spectra of anthracene–*o*-carborane dyad **100**. Reprinted with permission from ref 17. Copyright 2017 Wiley-VCH Verlag GmbH & Co. KGaA.

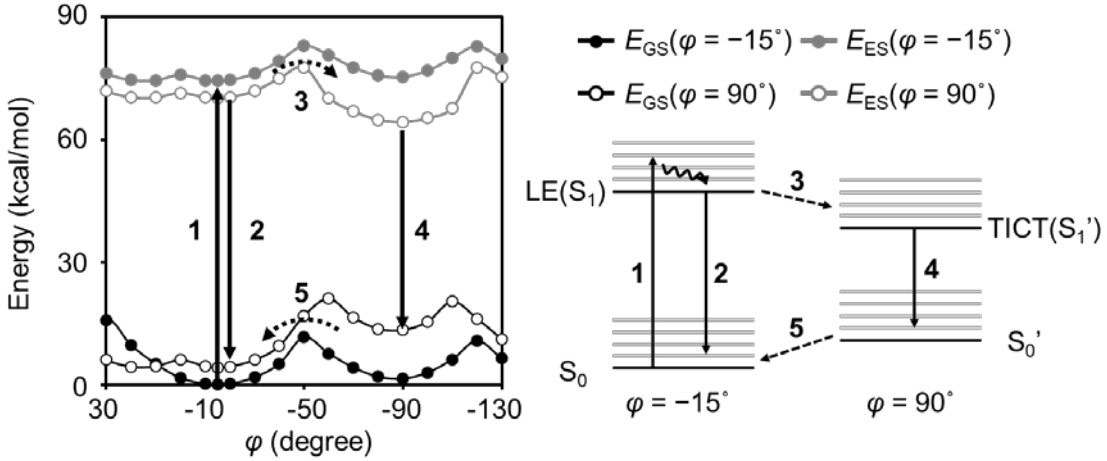

Figure 5. Calculation results with the anthracene–*o*-carborane dyad **100**. E_{GS} and E_{ES} represent energy in the ground and the excited states, respectively. The φ value means the angle between the C–C bond and the π-plane (φ = –15°: parallel, φ = 90°: perpendicular). Reprinted with permission from ref 17. Copyright 2017 Wiley-VCH Verlag GmbH & Co. KGaA.

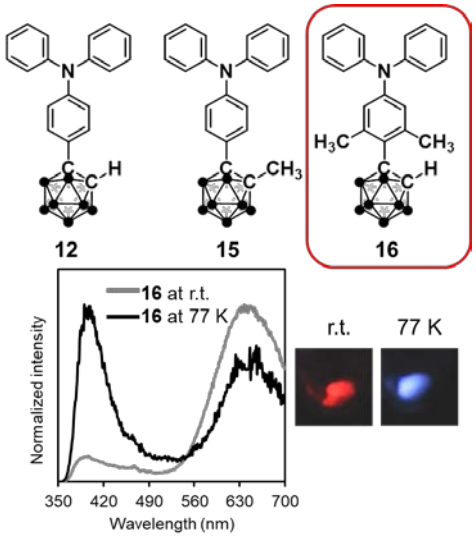

Figure 6. Chemical structures of TPA-substituted *o*-carboranes and representative emission spectra of **16** in solid at 77 K and ambient temperature. Reprinted with permission from ref 29. Copyright 2019 Wiley-VCH Verlag GmbH & Co. KGaA.

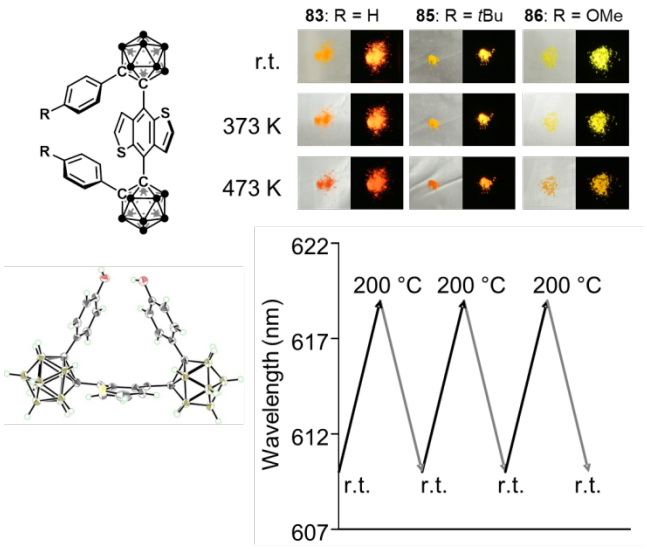

Figure 7. Rapid thermochromic luminescent properties of bis-*o*-carborane-substituted dithienylbenzenes. Reprinted with permission from ref 74. Copyright 2019 Wiley-VCH Verlag GmbH & Co. KGaA.

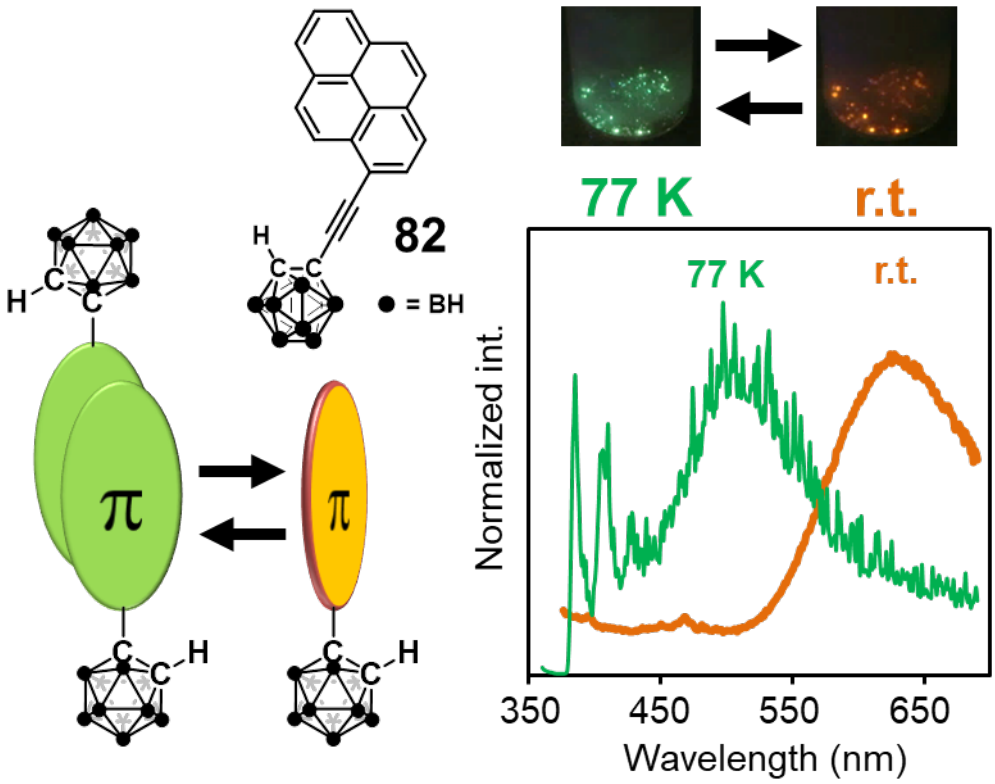

Figure 8. Chemical structure, luminescent spectra and plausible model for optical properties of the pyrene–*o*-carborane dyad **82** with the ethynyl spacer. Reprinted with permission from ref 64. Copyright 2017 Wiley-VCH Verlag GmbH & Co. KGaA.

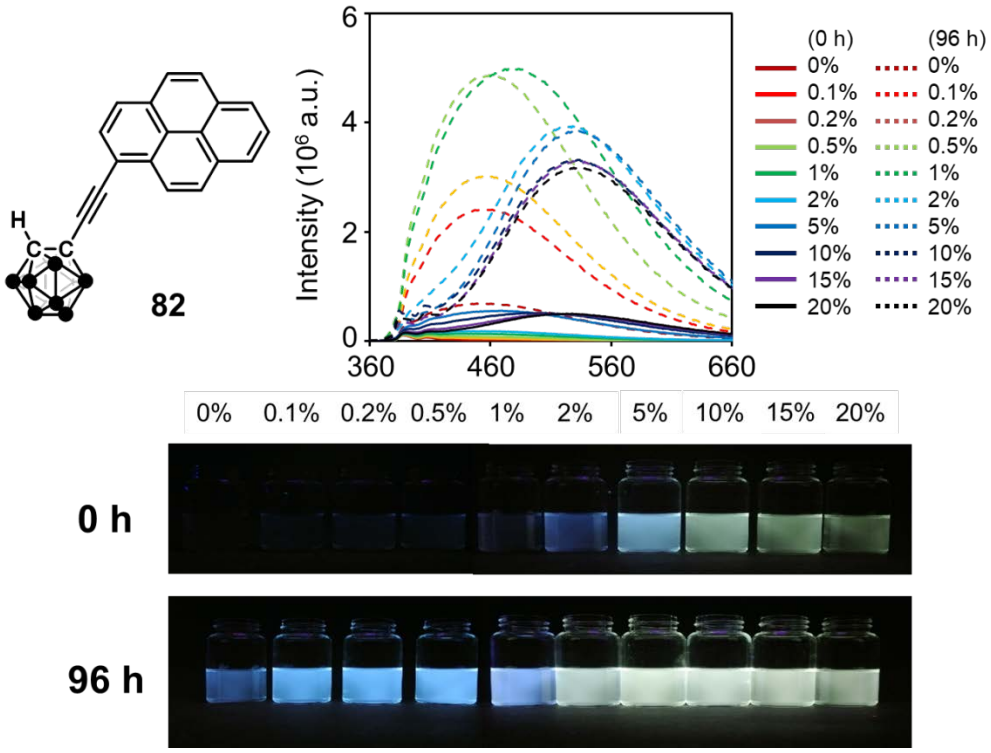

Figure 9. Luminescent spectra and pictures under UV light irradiation (365 nm) of the solution containing **82** in acetone with variable water contents before and after 96 h at 25 °C. Reprinted with permission from ref 65. Copyright 2019 Wiley-VCH Verlag GmbH & Co. KGaA.

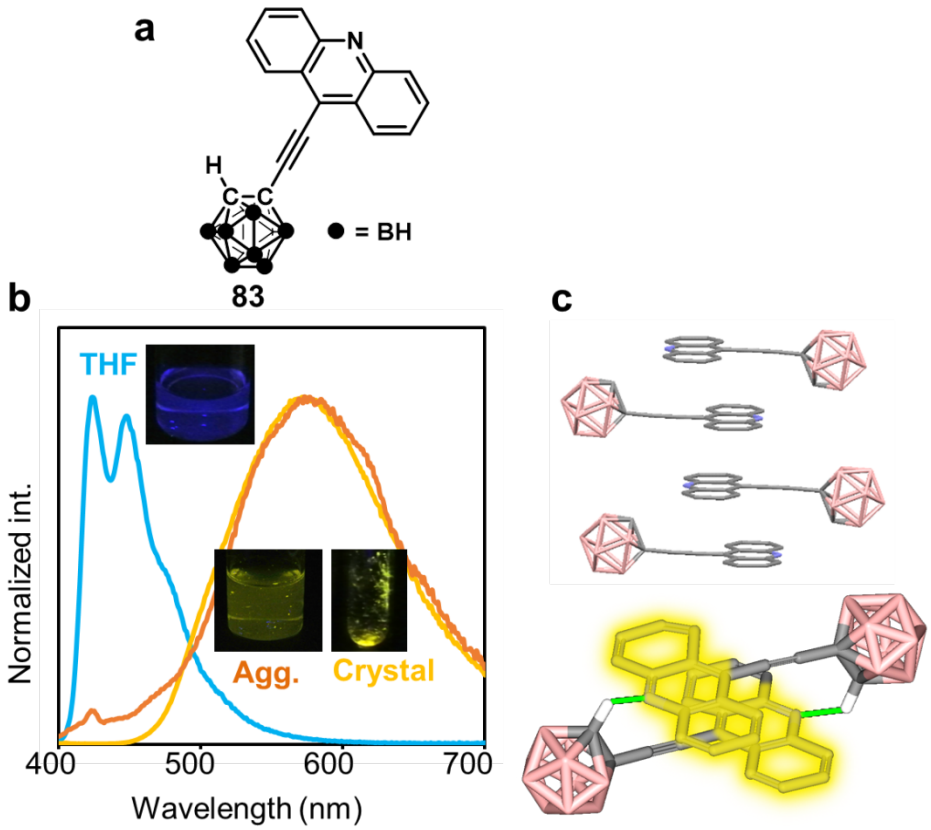

Figure 10. (a) Chemical structure, (b) luminescence spectra and (c) crystal packing of the acridine–*o*-carborane dyad **83** with the ethynyl spacer. Reprinted with permission from ref 66. Copyright 2019 Wiley-VCH Verlag GmbH & Co. KGaA.

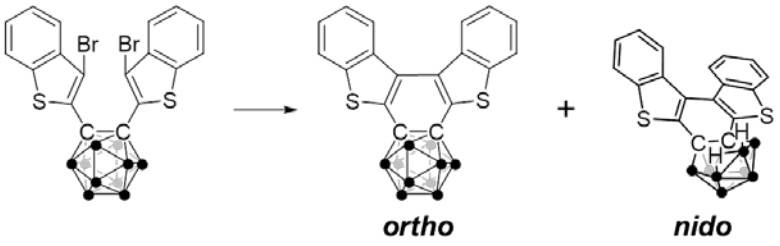

ortho ***nido***

	hexane		crystal		scratched	
	λ_{PL} (nm)	Φ_{PL}	λ_{PL} (nm)	Φ_{PL}	λ_{PL} (nm)	Φ_{PL}
ortho	376	<0.01	–	–	–	–
nido	521	0.64	556	0.49	547	0.57

Figure 11. Chemical structures and optical properties of *ortho*- and *nido*-carboranes.

GRAPHICAL ABSTRACT